Supporting information

Rapid field-ready electrical biosensor consisting of bismuthine-derived Au island decorated BiOCl nanosheets for *Raphidiopsis raciborskii* detection in freshwater

Hyunjun Park[a,†], Sun Woo Kim[b,†], Siyun Lee[a], Jeongyun An[a], Seokho Jung[a], Minju Lee[c], Jeonghyun Kim[c], Daeryul Kwon[d], Hongje Jang[b,*], and Taek Lee[a,*]

[a] *Department of Chemical Engineering, Kwangwoon University, 20 Gwangwoon-Ro, Nowon-Gu, Seoul 01897, Republic of Korea*

[b] *Department of Chemistry, Kwangwoon University, 20 Gwangwoon-Ro, Nowon-Gu, Seoul 01897, Republic of Korea*

[c] *Department of Electronics Convergence Engineering, Kwangwoon University, 20 Gwangwoon-Ro, Nowon-Gu, Seoul 01897, Republic of Korea*

[d] *Protist Research Division, Biological Resources Research Department, Nakdonggang National Institute of Biological Resources (NNIBR), 137, Donam 2-gil, Sangju-si, Gyeongsangbuk-do 37242, Republic of Korea*

† These authors contributed equally to this work

Corresponding Author

*Hongje Jang. Phone: +82-2-940-8320. E-mail: hjang@kw.ac.kr

*Taek Lee. Phone: +82-2-940-5771. E-mail: tlee@kw.ac.kr

Table of contents

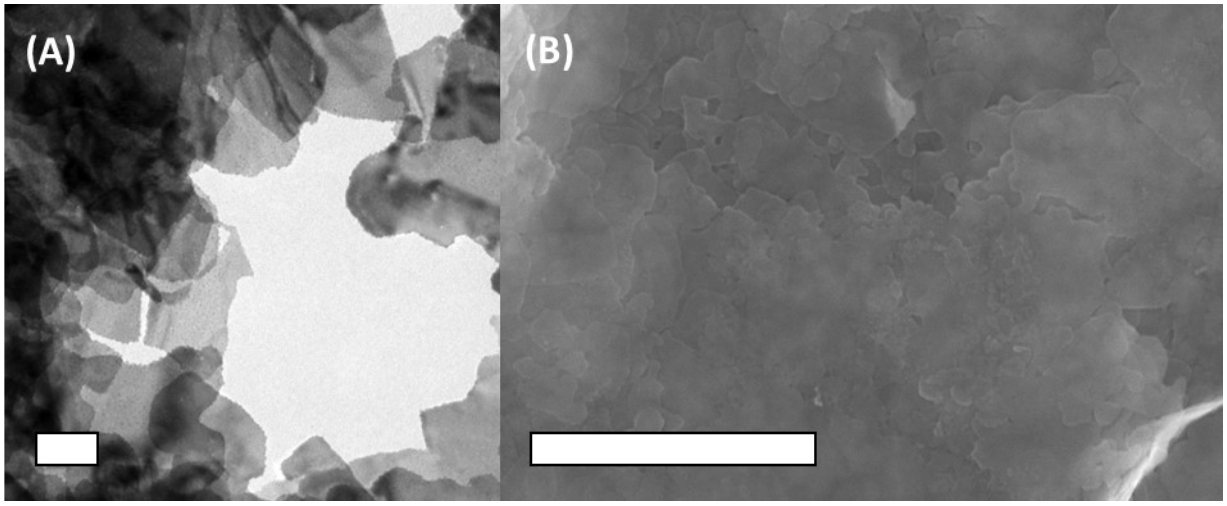

Figure S1. Electron microscopic characterization of synthesized bismuthene. (A) Transmission electron microscopy (TEM) and (B) scanning electron microscopy (SEM) image of bismuthene nanosheet. Scale bars = 500 nm.

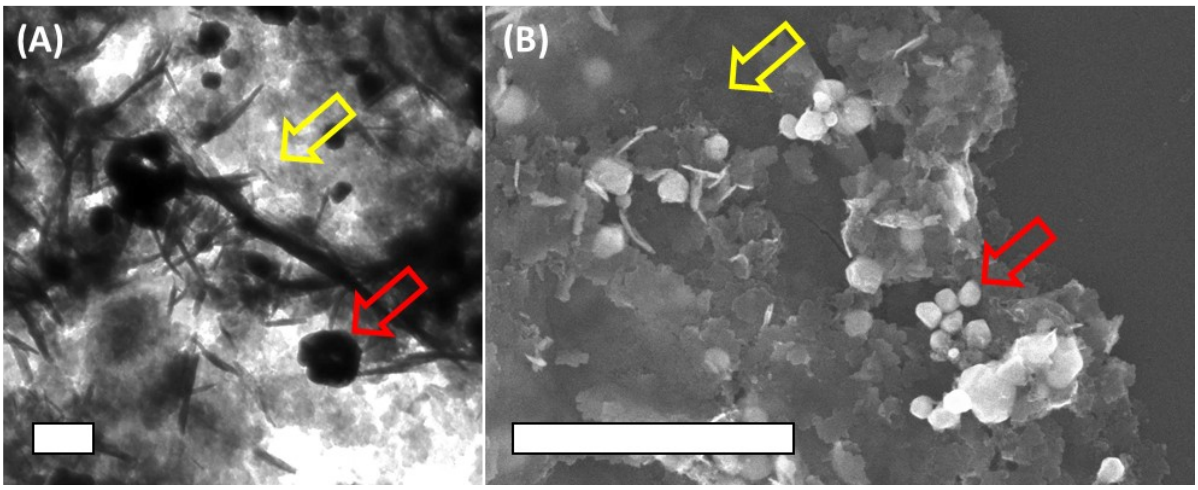

Figure S2. Lower magnification images for Au-BiOCl. (A) Transmission electron microscopy (TEM) and (B) scanning electron microscopy (SEM) images exhibited Au-BiOCl nanosheets (yellow arrow mark) and sparsely formed overgrown Au nanoparticles (red arrow mark). Scale bars = 500 nm.

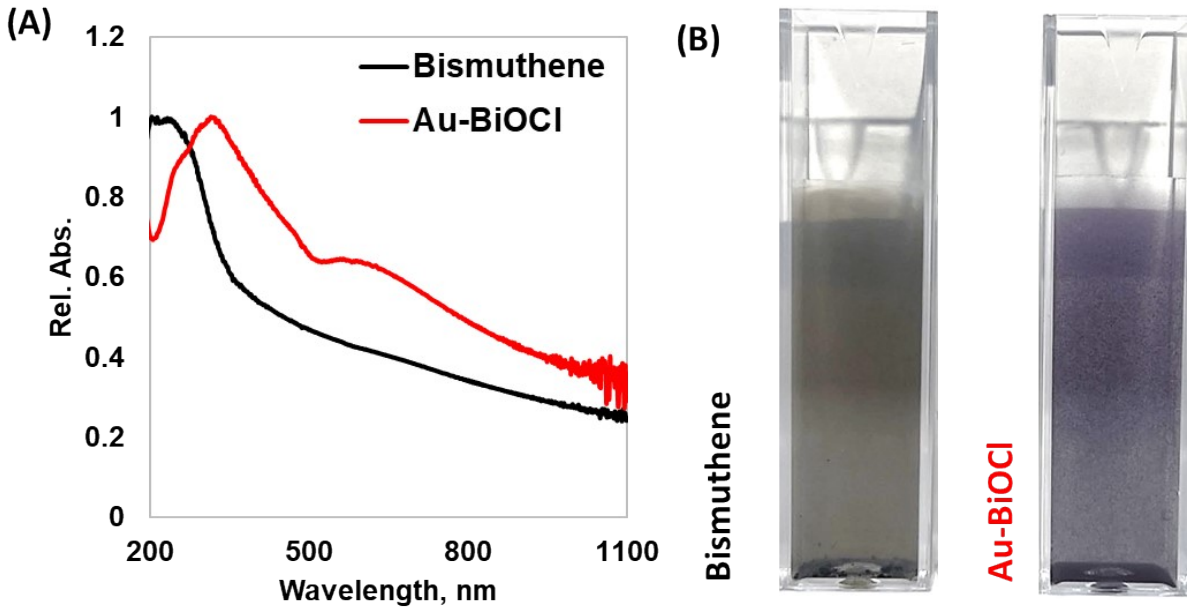

Figure S3. Optical characterization of bismuthene and Au-BiOCl. (A) Ultraviolet-visible-near infrared (UV-Vis-NIR) spectra and (B) digital photo image of bismuthene precursor and Au-BiOCl.

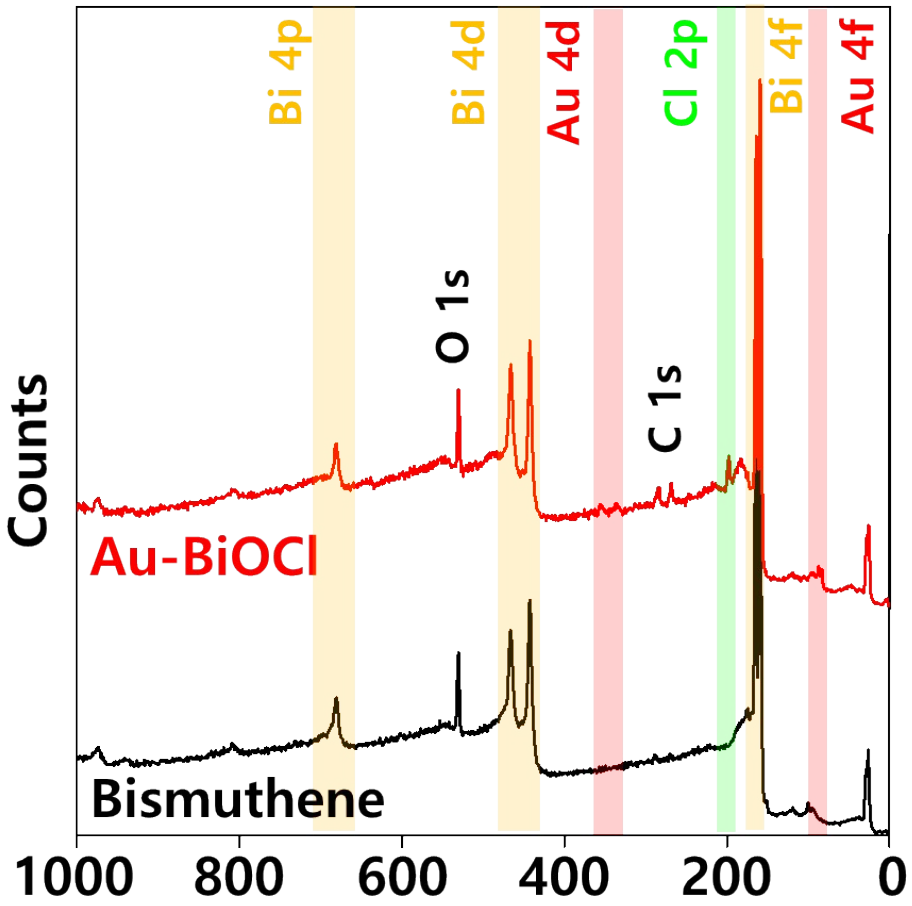

Figure S4. Wide scan X-ray photoelectron spectroscopy (XPS) spectra of bismuthene and Au-BiOCl.

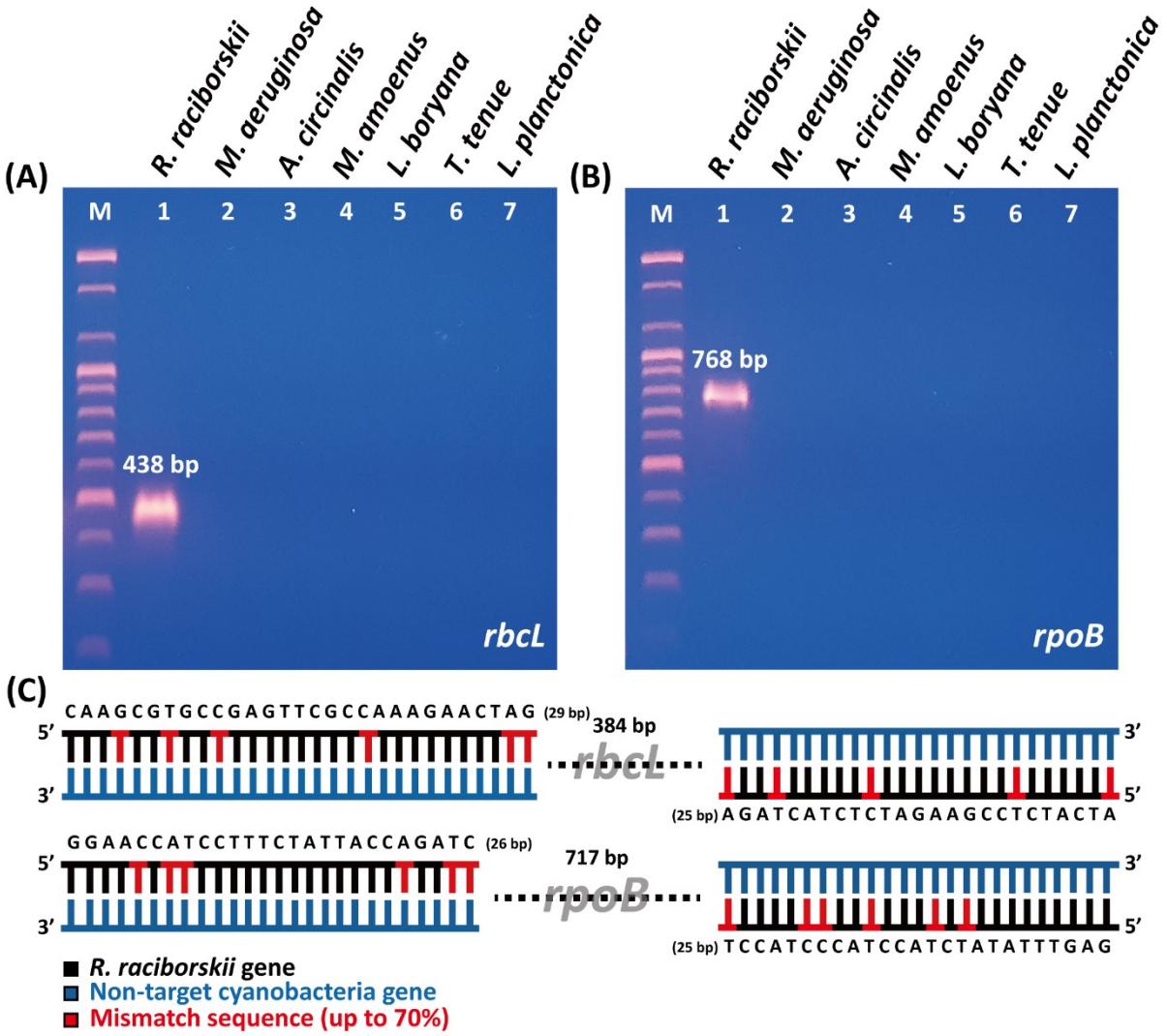

Figure S5. Polymerase chain reaction (PCR) results of 7 cyanobacteria DNAs, using the designed *Raphidiopsis raciborskii* specific (A) *RubisCO large subunit* (*rbcL*) and (B) *RNA polymerase beta subunit* (*rpoB*) probes. (C) The mismatched sequences of probe in *rbcL* and *rpoB* compared with non-target cyanobacteria DNA.

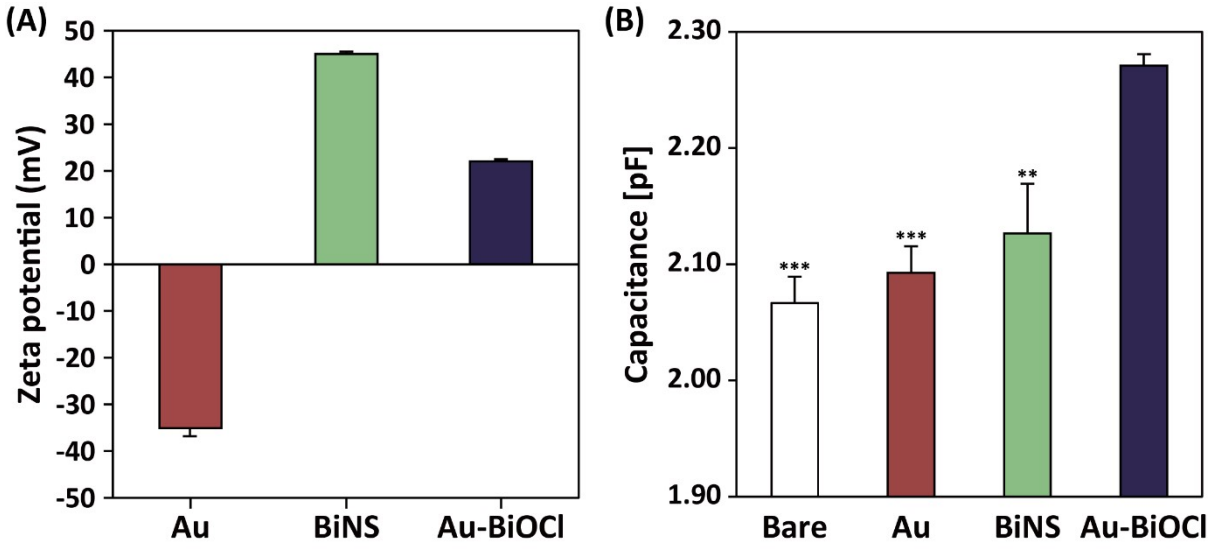

Figure S6. The (A) zeta potential and (B) capacitance results of Au nanoparticle, bismuth nanosheet (BiNS), and synthesized Au-BiOCl. Significant differences between the Au-BiOCl and single materials were determined by one-way analysis of variance (ANOVA) and are depicted as $^{**}p < 0.01$ and $^{***}p < 0.001$.

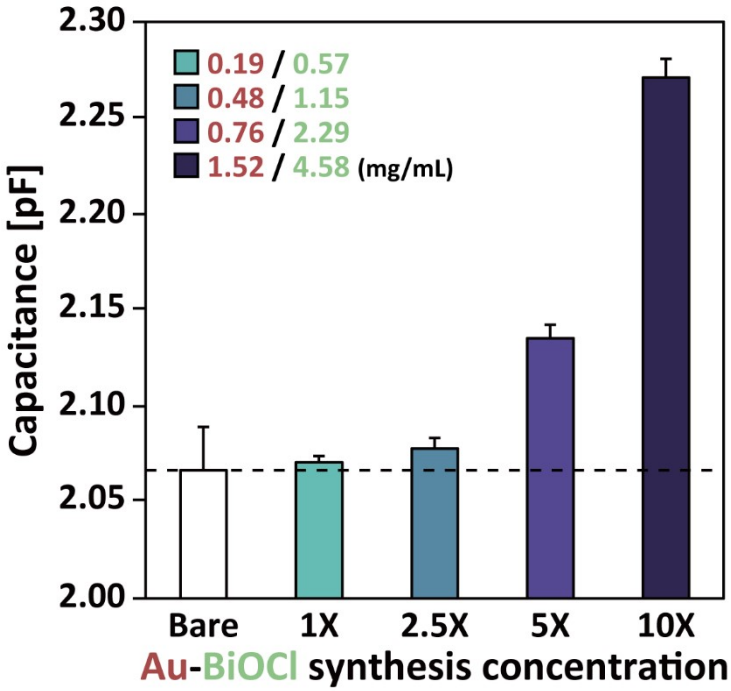

Figure S7. Capacitance value depending on Au-BiOCl synthesis concentration.

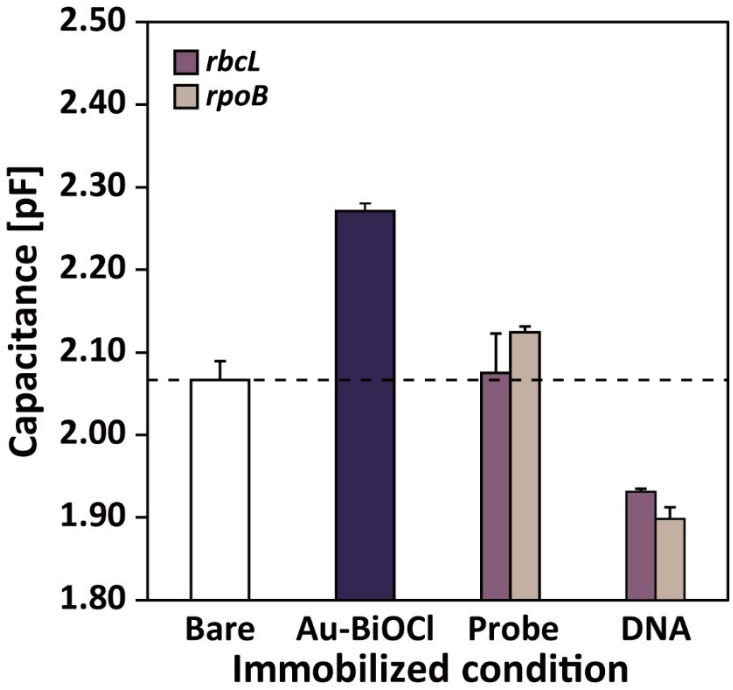

Figure S8. Capacitance trend at each stage of sensing membrane immobilization.

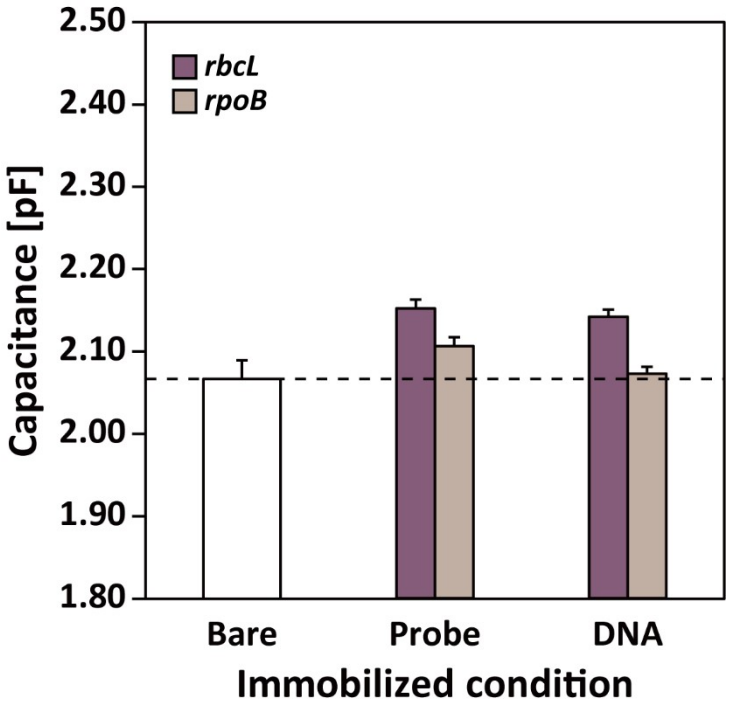

Figure S9. Capacitance measurement results without applying Au-BiOCl on the electrode at each immobilized stage in order of bare, probe, and target DNA.

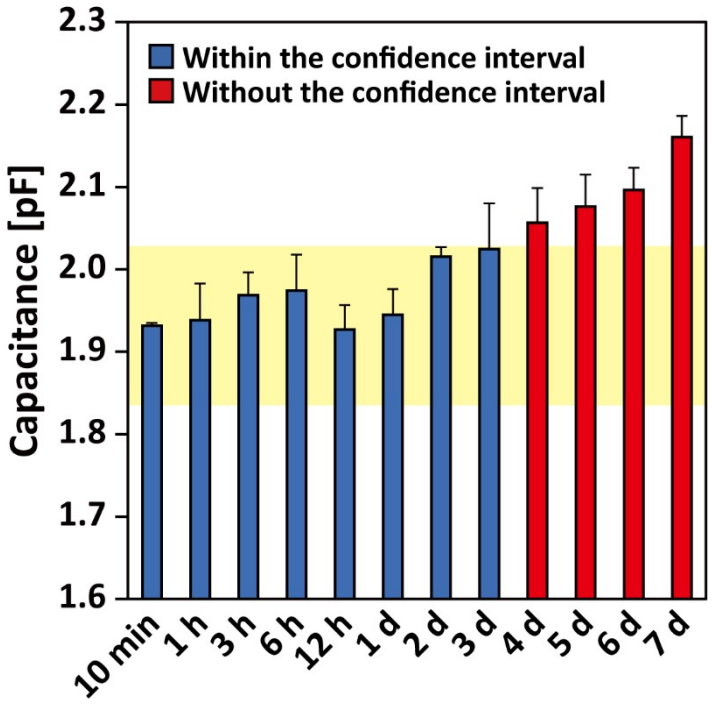

Figure S10. The stability of fabricated capacitive-type biosensor. Yellow box represented the electrical signal confidence level of ± 5 %.

Table S1. Harmful cyanobacteria species used in this study

Species name	Purpose	Strain code
Anabaena circinalis	Control group	FBCC-A104
Leptolyngbya boryana	Control group	FBCC-288
Limnothrix planctonica	Control group	FBCC-310
Microcoleus amoenus	Control group	FBCC-518
Microcystis aeruginosa	Control group	FBCC-A59
Raphidiopsis raciborskii	Target species	FBCC-A1229
Tychonema tenue	Control group	FBCC-324

Table S2. DNA sequence details used in the present study

Gene	Probe	Remark	Sequence
RubisCO large subunit (rbcL)	*R. raciborskii* rbcL-F	gDNA PCR	5'-CAA GCG TGC CGA GTT CGC CAA AGA ACT AG-3'
	R. raciborskii rbcL-R	gDNA PCR	5'-ATC ATC TCC GAA GAT CTC TAC TAG A-3'
	R. raciborskii rbcL probe	Biosensing	5' Thiol-CAA GCG TGC CGA GTT CGC CAA AGA ACT AG-3'
RNA polymerase beta subunit (*rpoB*)	*R. raciborskii* rpoB-F	gDNA PCR	5'-GGA ACC ATC CTT TCT ATT ACC AGA TC-3'
	R. raciborskii rpoB-R	gDNA PCR	5'-GAG TTT ATA TCT ACC TAC CCT ACC T-3'
	R. raciborskii rpoB probe	Biosensing	5' Thiol-GGA ACC ATC CTT TCT ATT ACC AGA TC-3'

Table S3. Species and GenBank accession numbers of non-specific cyanobacteria DNA sequences used for specific DNA probe design

Gene	Species	Accession number
RubisCO large subunit (*rbcL*)	*Raphidiopsis raciborskii*	CP091284
	Anabaena sp.	CP003284
	A. cylindrica	CP003659
	Anabaenopsis elenkinii	CP063311
	Dolichospermum sp.	CP043056
		CP050884
	Microcystis aeruginosa	AM157793
		CP089094
	Nodularia sphaerocarpa	CP060140
	N. spumigena	CP007203
RNA polymerase beta subunit (*rpoB*)	*Raphidiopsis raciborskii*	CP073250
	Aphanizomenon flos-aquae	CP051188
		CP051528
		JACJRO010000017
	Dolichospermum sp.	KI928194
		CP050882
		CP050884
		CP070233
	D. circinale	KE384612
		KE384713
	Nodularia sp.	REBL01000112
	N. spumigena	CP020114